

Study on thermal conductivity of periclase-hercynite bricks prepared from fused or sintered hercynite

Junhong Chen^{a*}, Mingwei Yan^a, Zhijian Li^b, Jindong Su^a, Bin Li^a and Jialin Sun^a

^aSchool of Materials Science and Engineering, University of Science and Technology Beijing, Beijing 100083, China

^bSchool of High Temperature Materials and Magnesium Resource Engineering, University of Science and Technology Liaoning, Anshan 114051, Liaoning, China

Periclase-hercynite bricks were prepared from fused or reaction-sintered hercynite. The microstructure of the obtained bricks was studied and their thermal conductivity in the simulated on-site condition was tested. The results show that the mutual diffusion of Fe or Al from hercynite and Mg from periclase forms more pores in the material. Compared with the brick prepared from fused hercynite, the brick from reaction-sintered hercynite has smaller pore size. The thermal conductivity simulation test of the two bricks at 1550 °C shows that the cold end temperature of the brick synthesized from the reaction-sintered hercynite is 40 °C lower than that of the brick from the fused hercynite. Thus, in consideration of reducing the shell temperature of the cement rotary kilns, the reaction-sintered hercynite is more favorable for the production of periclase-hercynite bricks.

Key words: Fused hercynite, Reaction-sintered hercynite, Microstructure, Thermal conductivity.

Introduction

Different with the lining of metallurgical furnaces such as ladles and converters in iron and steel industry, the refractories for the burning zone of cement rotary kilns are single-layered with a thickness of 180–220 mm. Besides the common functions, this layer of refractories shall ensure that the temperature of the kiln metal shell is under 350 °C although the temperature inside the kiln is at 1500 °C or above. Because when the metal shell temperature exceeds 300 °C, plastic flow happens: there is no obvious yield limit or yielding terrace in the stress-strain curve and the strength drops obviously. When the temperature is close to 400 °C, the strength of the metal structural pieces is nearly half of those at room temperature, which is very dangerous for rotary kiln operation [1].

The shell temperatures of the burning zone and transition zone of cement rotary kilns are relatively high, normally above 300 °C. If the refractories used in the positions have high thermal conductivity, or some bricks rupture because of the kiln shut down, or the refractories have small residual thickness, the shell temperature can achieve 350 °C or higher. So, high power fans are required to cool the shell on site. The characteristics of rotary kilns require refractories with low thermal conductivity and strong adaptability used

in the burning zone and transition zone of cement rotary kilns.

Currently, refractories used in the burning zone of rotary kilns are dolomite bricks, magnesia chrome bricks, magnesium aluminate spinel bricks, etc. [2–13] Magnesium aluminate spinel bricks have thermal conductivity of 3.5–5.0 W/(m·K) (350 °C)[14], which is relatively high among the oxides refractories. Dolomite bricks and magnesia chrome bricks have lower thermal conductivity but poor thermal shock resistance. The poor thermal shock resistance may lead to brick rupture during kiln shut down, raising temperature abruptly to 350 °C above.

In recent years, based on hercynite ($\text{FeO} \cdot \text{Al}_2\text{O}_3$) and periclase, periclase-hercynite refractories were developed [11, 13]. The developed periclase-hercynite refractories have excellent kiln coating ability, good structure flexibility and stress buffering ability, which results in the good performance in the burning zone of rotary kilns as a substitute for magnesia chrome bricks [15]. The periclase-hercynite refractories have become an important developing trend for chrome free refractories used in the burning zone of rotary kilns. In addition, compared with the magnesium aluminate spinel brick and magnesia chrome brick, the periclase-hercynite brick has lower thermal conductivity and better thermal shock resistance. So brick rupture happens rarely during kiln shut down. The performance the brick is stable and the shell temperature is relatively low.

As the raw material for the periclase-hercynite bricks, hercynite can be synthesized by reaction sintering or electric fusing. So the two kinds of periclase-hercynite

*Corresponding author:
Tel : +86-010-6233-2666
Fax: +86-010-6233-2666
E-mail: cjh2666@126.com

refractories can be prepared based on the two kinds of hercynite. Hercynite prepared by different methods has different crystal structures, namely different Fe^{2+} ions occupying and diffusing ability, resulting in different sensitivities to oxygen partial pressure. All these factors will influence the microstructure of the periclase-hercynite bricks, and further affect the thermal conductivity and other properties. So far, there is no report on this area.

To investigate the existing state of hercynite in the two periclase-hercynite bricks and the as-resulted thermal conductivity difference, this work contrasted with the structure of the two bricks and tested the thermal conductivity in the simulated on-site condition to provide data base for the application of the two kinds of bricks.

Experimental

The bricks were prepared using 12% (by mass) reaction-sintered hercynite (44% FeO and 56% Al_2O_3) or fused hercynite (44% FeO and 56% Al_2O_3) and 88% sintered magnesia (MgO 98%) as raw materials, pressing and firing at 1600 °C for 6 h. The brick prepared from fused hercynite (FH) is named FM brick and the brick prepared from sintered hercynite (SH) is named SM brick.

The phase composition of the two kinds of hercynite was characterized by an X-ray diffractometer (XRD; D8 ADVANCE) with the scanning time of 120 min and 2 θ range of 10 °-140 °. Based on Rietveld theory, the XRD patterns were refined by TOPAS software. The microstructure was investigated by a scanning electron microscope (SEM; Quanta200, FEI, Holland) equipped with an energy dispersive spectroscope (EDS; INCA250 Oxford Instrument, UK).

The device of the on-site simulation was a refit chamber high temperature electric furnace: two square holes with size of 55 mm × 55 mm × 160 mm were dug

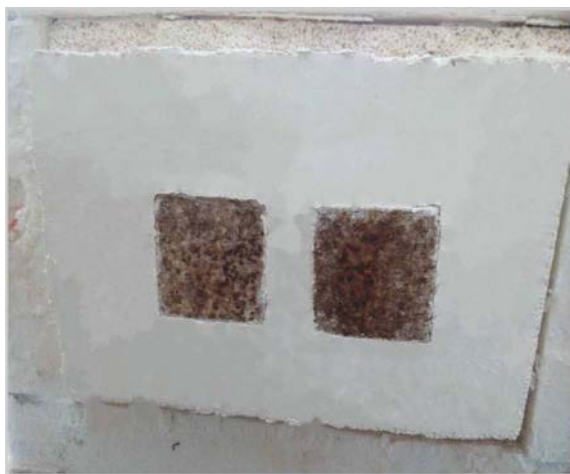


Fig. 1. On-site simulation for thermal conductivity test (FM brick at left side and SM brick at right side in the two images).

from the door of the electric furnace. The obtained bricks were cut into specimens with size of 55 mm × 55 mm × 160 mm. As shown in Fig. 1, the specimens were inserted into the hole and the gaps were filled with high temperature fiber felt to ensure the thermal flux runs through the specimens. After the installation, the furnace temperature was raised at a rate of 5 °C/min to 1550 °C. When the temperature reached and stayed at 1550 °C, the surface temperatures of the specimens were determined and recorded.

Results and Discussion

Fig. 2 shows the XRD patterns of the two kinds of hercynite. Their main compositions are both hercynite. The diffraction peaks of the fused hercynite moves rightwards compared with that of the sintered hercynite; and the fused hercynite has larger crystal parameters than the sintered hercynite.

Based on Rietveld refinement theory and TOPAS software, the crystal parameters and atom occupancy of the two kinds of hercynite were calculated, as shown in Fig. 3. After refinement, the structural formulas were given: for fused hercynite and for reaction-sintered hercynite. As shown by the structural formulas, the fused hercynite has more Fe^{2+} in the tetrahedron sites, so the fused hercynite is more stable in the oxidation atmosphere [16].

The XRD and Rietveld refinement of the two kinds of hercynite show that although they have similar diffraction peaks, the atom structure and atom occupancy are different, which leads to different properties.

SEM images of the two kinds of hercynite are shown in Fig. 4. Different morphologies can be observed. The fused hercynite has larger crystal grains, hundreds of micron meters mostly; while the reaction-sintered hercynite has smaller crystal grains mostly under 40 μm .

The SEM images of the hercynite in the two bricks are shown in Fig. 5. After firing, the microstructure of the two bricks changes differently. Hercynite particles are still observed in the FM brick. While the microstructure of the SM brick changes greatly. Large

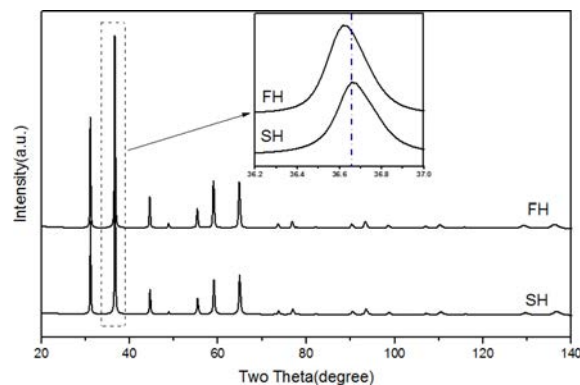


Fig. 2. XRD patterns of the two kinds of hercynite.

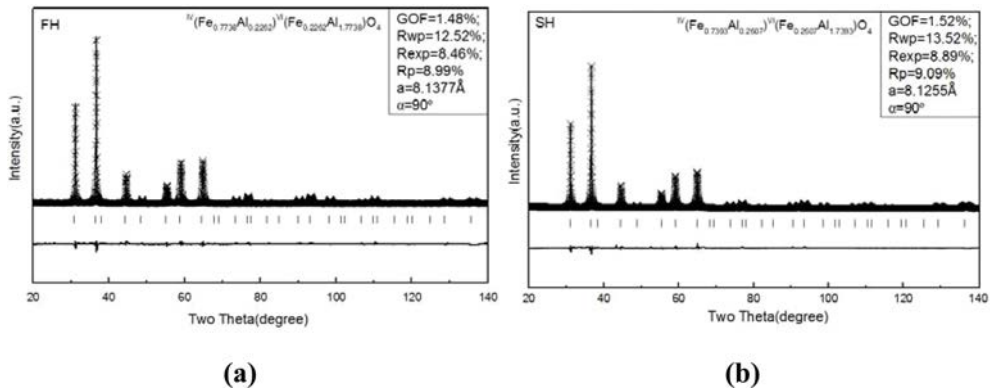


Fig. 3. XRD refinement of the two kinds of hercynite.

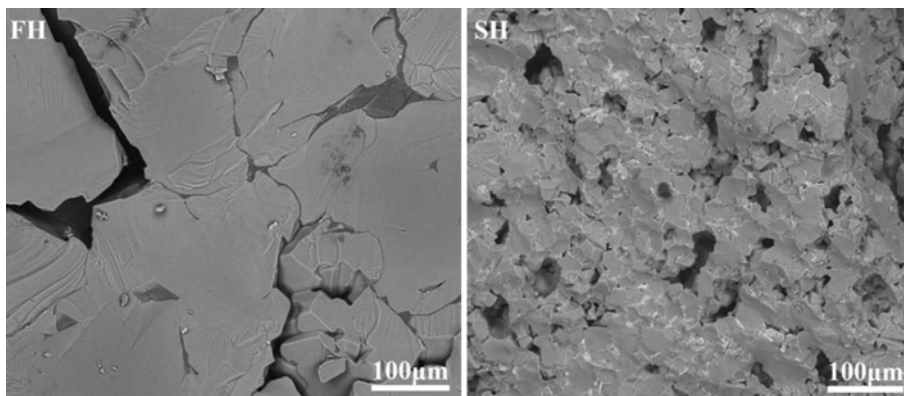
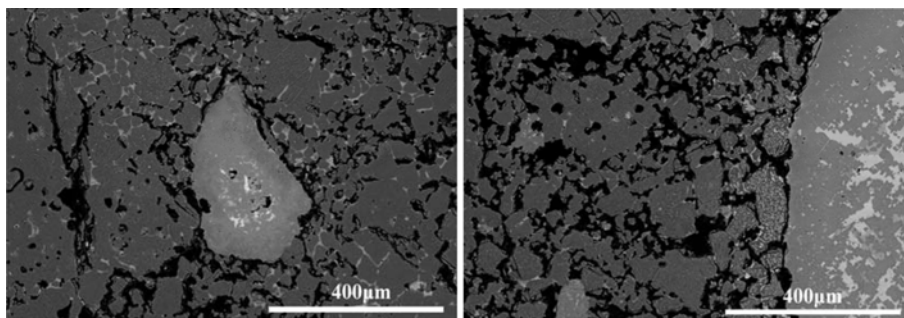
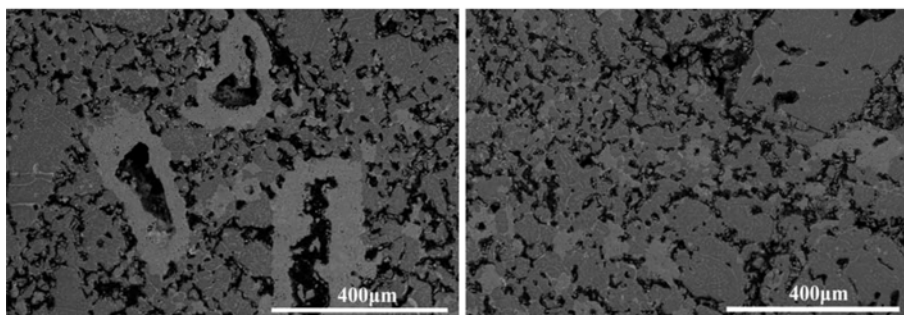


Fig. 4. SEM images of the two kinds of hercynite.



(a) SEM images of FM brick



(b) SEM images of SM brick

Fig. 5. SEM images of the two periclase-hercynite bricks.

holes appear in original hercynite grains and many micro cracks appear in the matrix. Moreover, the magnesia

around the sintered hercynite changes greatly: it is obviously brighter than the other magnesia. While the

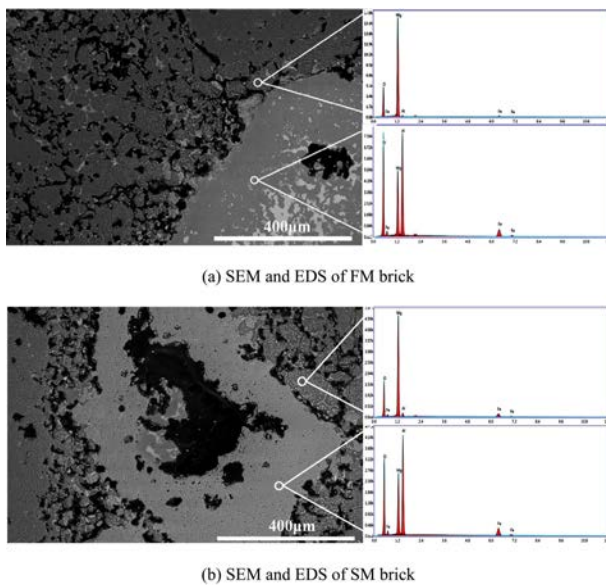


Fig. 6. SEM and EDS of the two periclase-hercynite bricks.

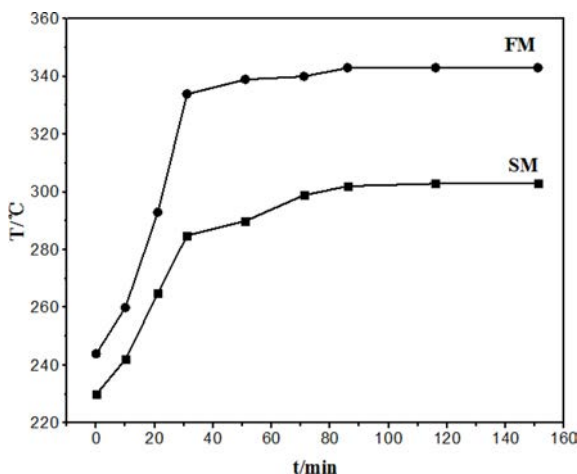


Fig. 7. Cold end temperature of the two bricks over time with furnace temperature held at 1550 °C

magnesia around the fused hercynite changes relatively less.

The further characterization and analysis of the structure around the hercynite are shown in Fig. 6. Many bright spots are observed in the periclase grains which contact the hercynite grains. The EDS result shows that the bright spots are composed of Mg, Fe, Al and O; while the hercynite is composed of Mg, Fe, Al and O. This means that the mutual diffusion happens between hercynite and periclase: Mg enters hercynite while Fe and Al enter periclase.

The cold end temperature changes of the two bricks over time when the furnace temperature was held at 1550 °C are shown in Fig. 7. The cold end temperatures of the two bricks in equilibrium are 303 °C and 343 °C respectively, indicating their different thermal conductivities. The SM brick has lower thermal conductivity, which is important for controlling the shell temperature at the kiln coating

stage in the beginning.

Fused hercynite was synthesized by heating ferric oxides and alumina to the melting state and then cooling at specified rate to make hercynite crystallize gradually. While the reaction-sintered hercynite was synthesized at the temperature lower than the melting point of hercynite through the ion mutual diffusion and migration between ferric oxides and alumina. According to the mass transfer theory, the mass transfer resistance is big in solid and small in liquid. Therefore, compared with the sintered hercynite, the fused one has smaller crystallization resistance, better crystal growth, and better crystal stability. The SEM images in Fig. 4 show that the fused hercynite grains are much bigger than the sintered hercynite grains, and the XRD refinement confirms the better stability of fused hercynite.

At 1600 °C in air, because of the existence of oxygen, Fe^{2+} in the hercynite surface is transformed into Fe^{3+} : $4\text{O}_2 \rightarrow 4\text{O}_\text{o}^{\times} + 2\text{V}_\text{M}^{\text{III}} + \text{V}_\text{T}^{\text{II}} + 8\text{h}^{\square}$ [17], increasing concentrations of octahedron vacancies and tetrahedron vacancies, so the outward diffusion abilities of Fe and Al are enhanced. Moreover, Fe^{2+} (or Fe^{3+}) and Al^{3+} in hercynite diffuse towards periclase and Mg^{2+} in magnesia moves towards hercynite. Fe^{2+} (or Fe^{3+}), and Al^{3+} diffuse faster than Mg^{2+} , producing Tyndall effect and resulting in cavities inside the hercynite. On the shell wall of the cavities, a composite spinel layer is formed. Besides the changes of hercynite grains and magnesia grains, the hercynite fines in the matrix also change greatly. The hercynite fines and magnesia fines are sintered together at high temperatures and a lot of micropores form because of the ion mutual diffusion between periclase and hercynite.

Compared with the fused hercynite, the sintered hercynite has smaller crystal size, worse structure stability, and less Fe^{2+} in tetrahedron sites, so during the preparation of periclase-hercynite bricks, the sintered hercynite is easy to be oxidized into Fe^{3+} , producing high concentration vacancies. Moreover it has lower crystal lattice diffusion activation energy. Therefore, the sintered hercynite reacts with the surrounding magnesia particles or fines more severely, forming more micropores (Fig. 5) which result in the lower thermal conductivity, thus it is more suitable for the burning zone of rotary kilns.

Summary

The microstructure of two kinds of periclase-hercynite bricks prepared from fused hercynite and reaction sintered hercynite, respectively was studied and their thermal conductivity were investigated at the simulated on-site condition. The results show that mutual diffusion happens during high temperature firing of the two bricks. Fe and Al in hercynite diffuse into magnesia and Mg in magnesia diffuses into hercynite, forming pores. Compared with the brick synthesized from fused hercynite, the brick

synthesized from sintered hercynite has smaller micro cracks. The thermal conductivity test at the simulated condition shows the cold end temperature of the brick synthesized from sintered hercynite is about 40 °C lower than that of the brick synthesized with fused hercynite. Therefore, the periclase-hercynite brick synthesized from the sintered hercynite is more suitable for the burning zone of rotary kilns.

Acknowledgments

The authors express their appreciation to National Nature Science Foundation of China of No. 51172021, and the National Science-technology Support Plan Projects (Grant 2013BAF09B01).

References

1. R.Y. Wei, J. Fujian College of Architecture & C. E. 4 (2002) 5-9.
2. J.L. Rodríguez, M.A. Rodríguez, S. De Aza and P. Pena, J. Eur. Ceram. Soc. 21[3] (2001) 343-354.
3. H. Kosuka, Y. Kajita, Y. Tuchiya, T. Honda and S. Ohta, in Proceedings of Third UNITECR'93. ALAFAR-Asociación Latinoamericana de Fabricantes de Refractories (Sao Paulo, Brazil, 1993) p. 1021-1037.
4. M. Chen, C. Lu and J. Yu, J. Eur. Ceram. Soc. 27[16] (2007) 4633-4638.
5. S. Serena, M.A. Sainz and A. Caballero, J. Eur. Ceram. Soc. 29[11] (2009) 2199-2209.
6. Z. Guo, S. Palco and M. Rigaud, J. Am. Ceram. Soc. 88[6] (2005) 1481-1487.
7. G.E. Goncalves, A.K. Duarte, and P.O.R.C. Brant, Am. Ceram. Soc. Bull. 72 (1993) 49-54.
8. J.L. Rodríguez, M.A. Rodríguez, S. De Aza and P. Pena, J. Eur. Ceram. Soc. 21[2] (2001) 343-354.
9. E.A. Rodríguez, G.A. Castillo, T.K. Das, R. Puente-Ornelas, Y. González, A. M. Arato and J.A. Aguilar-Martínez, J. Eur. Ceram. Soc. 33[14] (2013) 2767-2774.
10. G.P. Liu, N. Li, Y. Wang, G.H. Gao, W. Zhou and Y.Y. Li, J. Ceram. Process. Res. 13 (2012) 480-485.
11. G.P. Liu, N. Li, Y. Wang, C.H. Tao, W. Zhou, and Y.Y. Li, Ceram. Int. 40[7] (2014) 8149-8155.
12. G. Buchebner, T. Molinari and H. Harmuth, in Proceedings of 6th UNITECR'99, (Berlin, Germany, 1999) p. 201-203.
13. J. Nievoll, Z. Q. Guo and S. Shi, RHI Bulletin. 3 (2006) 15-17.
14. L. Yuan, J.Z. Wang, X.F. Chen, and L.L. Zhang, China Cement. 3 (2006) 70-73.
15. J.H. Chen, L.Y. Yu, J.L. Sun, Y. Li, and X. D. Xue, J. Eur. Ceram. Soc. 31[3] (2011) 259-263.
16. R. Freer and W. O' Reilly, Mineral. Mag. 43 (1980) 889-899.
17. B. Lavina, F. Princivalle, and A.D. Giusta, Phys. Chem. Minerals. 32[2] (2005) 83-88.